The Astrophysical Journal, 736:54 (10pp), 2011 July 20 doi:10.1088/0004-637X/736/1/54

SPITZER OBSERVATIONS OF GX17+2: CONFIRMATION OF A PERIODIC SYNCHROTRON SOURCE

Thomas E. Harrison[1], Bernard J. McNamara[1], Jillian Bornak[1], Dawn M. Gelino[2], Stefanie Wachter[3], Michael P. Rupen[4], and Christopher R. Gelino[5]
[1] Department of Astronomy, New Mexico State University, Las Cruces, NM 88003-8001, USA; tharriso@nmsu.edu, bmcnamar@nmsu.edu, jbornak@nmsu.edu
[2] NASA Exoplanet Science Institute, California Institute of Technology, Pasadena, CA 91125, USA; dawn@ipac.caltech.edu
[3] Spitzer Science Center, Caltech M/S 220-6, Pasadena, CA 91125, USA; wachter@ipac.caltech.edu
[4] National Radio Astronomy Observatory, Socorro, NM 87801, USA; mrupen@aoc.nrao.edu
[5] Infrared Processing and Analysis Center, Caltech M/S 220-6, Pasadena, CA 91125, USA; cgelino@ipac.caltech.edu
Received 2011 February 16; accepted 2011 May 4; published 2011 July 6

ABSTRACT

GX17+2 is a low-mass X-ray binary (LMXB) that is also a member of a small family of LMXBs known as "Z-sources" that are believed to have persistent X-ray luminosities that are very close to the Eddington limit. GX17+2 is highly variable at both radio and X-ray frequencies, a feature common to Z-sources. What sets GX17+2 apart is its dramatic variability in the near-infrared, where it changes by $\Delta K \sim 3$ mag. Previous investigations have shown that these brightenings are periodic, recurring every 3.01 days. Given its high extinction ($A_V \geqslant 9$ mag), it has not been possible to ascertain the nature of these events with ground-based observations. We report mid-infrared *Spitzer* observations of GX17+2 which indicate a synchrotron spectrum for the infrared brightenings. In addition, GX17+2 is highly variable in the mid-infrared during these events. The combination of the large-scale outbursts, the presence of a synchrotron spectrum, and the dramatic variability in the mid-infrared suggest that the infrared brightening events are due to the periodic transit of a synchrotron jet across our line of sight. An analysis of both new, and archival, infrared observations has led us to revise the period for these events to 3.0367 days. We also present new *Rossi X-Ray Timing Explorer* (*RXTE*) data for GX17+2 obtained during two predicted infrared brightening events. Analysis of these new data, and data from the *RXTE* archive, indicates that there is no correlation between the X-ray behavior of this source and the observed infrared brightenings. We examine various scenarios that might produce periodic jet emission.

Key words: infrared: stars – stars: individual (GX17+2) – stars: neutron – X-rays: binaries

1. INTRODUCTION

GX17+2 is a low-mass X-ray binary (LMXB) that is also a member of the small family of objects called "Z-sources." In Z-sources, the neutron star primary is accreting mass at a rate that is close to the Eddington limit. Z-sources are among the most luminous, persistent X-ray sources in the Galaxy. The Z-like pattern (see Section 4) traced in an X-ray color–color diagram has been associated with a changing accretion rate for these sources (Hasinger et al. 1990; Vrtilek et al. 1990). Recently, however, this simple scenario has been losing favor. For example, Jackson et al. (2009) propose that changes in the mass accretion rate and neutron star temperature drive motion along the normal branch (NB). The increasing temperature along the NB eventually increases the radiation pressure to such a point that the inner disk is disrupted, leading to jet formation. They also propose that unstable nuclear burning occurs on the flaring branch (FB). In contrast, Lin et al. (2009) have proposed that the various branches of the Z have less to do with the accretion rate and more to do with the structure of the accretion disk. They believe that the mass accretion rate is nearly constant throughout the Z, and that motion along the NB is due to a changing boundary layer. The horizontal branch (HB) results from Comptonization of disk emission, and the FB is due to a changing/variable inner disk radius, but at a nearly constant accretion rate.

In addition to their changing X-ray emission, Z-sources also exhibit highly variable radio emission. This radio emission is attributed to synchrotron jets, and radio jets have now been clearly detected in several Z-sources, including the subject of this paper: GX17+2 (Migliari et al. 2007). Penninx et al. (1988) found that the radio emission from GX17+2 was the most intense when the source was on the HB. Migliari & Fender (2006) believe that this correlation is due to the formation/presence of a compact jet on the HB, and that radio emission, including optically thin synchrotron flares, accompany the transition from the HB to the NB. They find that there is no significant radio emission when GX17+2 is on the FB. In addition, a hard X-ray tail is present on the HB (Di Salvo et al. 2000) when the source has its highest radio fluxes. These results clearly indicate that a relativistic jet is often present in this source.

Identification of the optical counterpart to GX17+2 long remained confused with a non-variable field star (NP Ser), even though radio observations clearly demonstrated that this star was not consistent with the position of this source (see Deutsch et al. 1999 for a full discussion). It was only when Callanan et al. (2002) observed a sudden brightening in the *K* band of an object near NP Ser that the true "optical" counterpart to GX17+2 was found. Surprisingly, this object appears to change by $\Delta K \approx 3$ mag. Callanan et al. (2002) examined scenarios to explain this variability and concluded that synchrotron emission was the most likely cause for these large-scale events. To examine the duty cycle of the infrared brightenings, Bornak et al. (2009, hereafter "Paper I") presented the data from a campaign on this source which revealed the unexpected result that these brightening events repeated every 3.01 days. During these events, the source could stay bright for many hours. Given the large extinction to GX17+2, and its relative faintness, it has not been possible to obtain sufficient ground-based observations of this source to enable us to conclusively identify the nature

Table 1
Spitzer Observation Log

Request Key	Start Time (UT)	End Time (UT)	Wavelength	Exp. Time (s)	No. of Images
26687744	2008 May 10 04:48:54	2008 May 10 04:52:20	4.5/8.0	0.6/10.4	11/11
26686720	2008 Oct 21 06:08:19	2008 Oct 21 07:03:28	24	9.96	288
34781184	2009 Oct 20 16:58:38	2009 Oct 20 18:46:26	3.6/4.5	2.00	720/720
35303680	2009 Nov 1 17:57:31	2009 Nov 1 19:45:19	3.6/4.5	2.00	720/720

of these *K*-band brightening events. Thus, we have turned to the *Spitzer* observatory to obtain longer-wavelength data. These observations reveal a spectral energy distribution (SED) during "outburst" that is consistent with a synchrotron source. We discuss our observations in the following section, present our results in Section 3, discuss possible interpretations for this variability in Section 4, and list our conclusions in Section 5.

2. OBSERVATIONS

While the thrust of this program revolves around new *Spitzer Space Telescope* observations, we have continued to monitor GX17+2 in the near-IR to further constrain its ephemeris. In addition, we have obtained simultaneous *Rossi X-Ray Timing Explorer* (*RXTE*) observations during two predicted *K*-band brightening events to explore whether the X-ray emission might be correlated with the *K*-band activity. We discuss the reduction of these various data sets here.

2.1. Spitzer Observations

We presented an ephemeris for the *K*-band brightenings of this source in Paper I. We used this ephemeris to schedule the observations of this object. The *Spitzer Space Telescope* is equipped with two instruments that obtained imaging data in multiple bandpasses: IRAC (Fazio et al. 2004) and MIPS (Rieke et al. 2004). During the cryogenic phase of the mission, IRAC obtained data in four bandpasses, 3.6, 4.5, 5.8, and 8 μm, while MIPS obtained imaging data at 24, 70, and 160 μm. Before the ephemeris was finalized, GX17+2 was observed with IRAC (G0 50670; PI: D. Gelino) on 2008 May 10. The ephemeris for GX17+2 predicted that it would not have been infrared bright at this time. By the time the MIPS photometry portion of the program was being scheduled, we were able to adjust the timing of those observations to allow them to occur during an outburst (2008 October 21). During the post-cryo phase of the mission, we (GO 60086; PI: T. E. Harrison) obtained two epochs of observation using IRAC during predicted brightenings: 2009 October 20 and 2009 November 1. The *Spitzer* observation log is presented in Table 1.

The IRAC and MIPS data were reduced using MOPEX, specifically the "APEX multi-frame" procedure as outlined in the Mopex Users Guide.[6] Note that for the first epoch (4.5 and 8.0 μm) IRAC observations, when GX17+2 was in a faint state, only the field star NP Ser was visible, and then only in the 4.5 μm bandpass. For the post-cryo IRAC observations, both the 3.6 and 4.5 μm observations spanned nearly an hour, allowing for the extraction of a light curve besides the single epoch fluxes in each bandpass obtained with MOPEX. We used IRAF to extract these light curves by first producing a median "sky" frame for each bandpass that was then subtracted from each of the images (there were 720 images per bandpass). We then performed differential aperture photometry on GX17+2 and several field stars to produce light curves (see Section 3.1).

[6] The MOPEX User's Guide can be found at http://ssc.spitzer.caltech.edu/dataanalysistools/tools/mopex/mopexusersguide/home/.

2.2. Near-infrared Photometry

We employed the Near-infrared Camera and Fabry-Perot Spectrometer ("NICFPS") on the Apache Point Observatory 3.5 m telescope to obtain *H*- and *K*-band photometry of GX17+2 on 2010 May 18 and 2010 May 24. NICFPS has a 1024 square HgCdTe array with a pixel scale of 0.273 arcsec pixel^{-1}. Due to the crowded field near GX17+2, a five-point dither pattern was used, allowing for the formation of a median sky frame that was then subtracted from each image. Aperture photometry was then performed on GX17+2 and four nearby field stars to produce differential photometry that was then calibrated using the 2MASS data for these stars. On May 18, GX17+2 was observed continuously from 07:46 UT to 11:08 UT. On May 24, only two short data sets were obtained, one centered at 07:43 UT and the other centered at 09:53 UT.

We presented an ephemeris for this source in Paper I, where a best-fitting period near 3.01 days was found. Given the sparse observational data set, several other periods near this value had similar probabilities (see Figure 2 in Paper I). By inclusion of the new *Spitzer* observations detailed in Table 1, and the outburst observations tabulated in Paper I, it was clear that a period near 3.03 days was slightly better at fitting the entire set of observed events. This revised ephemeris was projected forward to predict that three more events were well timed for observations from the Apache Point Observatory: 2010 May 18, 21, and 24. Unexpectedly, however, no brightening occurred on May 18. The event on May 21 was not observed. On May 24, however, GX17+2 was again apparent. In Figure 1, we present NICFPS *K*-band images for both nights. GX17+2 is located about 1″ north of the field star NP Ser. On May 24, the presence of GX17+2 adds an elongated appearance to NP Ser. Comparison of the photometry finds that on May 24 the blend of NP Ser and GX17+2 were brighter by $\Delta K = 0.39$ and $\Delta H = 0.10$ mag than on May 18. In fact, the *H*- and *K*-band magnitudes of NP Ser on May 18 ($H_{\rm 2MASS} = 14.56$, $K_{\rm 2MASS} = 14.43$) were identical to all of the previous non-outburst observations of this source. This is the first time we have not detected a predicted outburst of GX17+2. As we discuss below, simultaneous *RXTE* observations reveal that GX17+2 was on the FB at this time.

2.3. RXTE Observations

As noted in Paper I, the 2006 July 12 event had simultaneous X-ray observations obtained using *RXTE*. We also scheduled *RXTE* observations for the May 18 and 21 brightenings noted above. The 2006 July 12 data set spanned the interval 08:59–09:33 UT. On 2010 May 18, GX17+2 was observed from 03:19 to 15:09 UT. On 2010 May 21, it was observed from 03:32 to 17:02 UT. All of these data were obtained in "Std2" mode which gives a temporal resolution of 16 s and 129 spectral channels. We have generated light curves from the *RXTE*

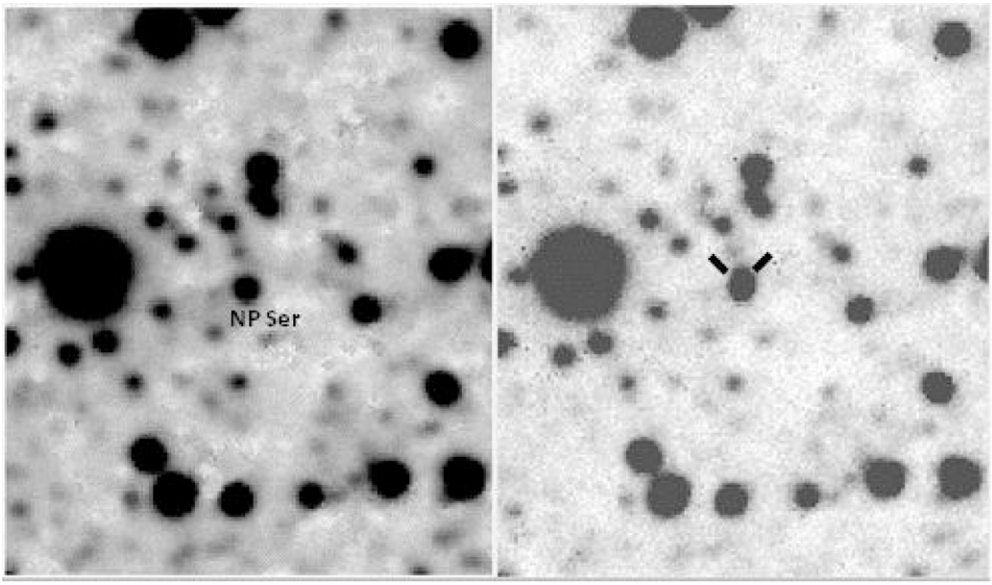

Figure 1. *K*-band images of the field of GX17+2 on 2010 May 18 (left) and 2010 May 24 (right). The field star NP Ser is labeled in the left-hand frame and, at this pixel scale, becomes slightly elongated to the north (tick marks) when GX17+2 is bright (May 24). North is up and east is to the left in these images that span approximately 30″ on each side.

"standard products"[7] data files. The light curves for the three lowest energy, standard product bands (2–4 keV, 4–9 keV, and 9–20 keV), as well as the hardness ratio (defined as the 4–9 keV count rate ("Channel 2") divided by the 2–4 keV count rate ("Channel 1")) for 2006 July 12, 2010 May 18, and 2010 May 21 are presented in Figure 2. The ratio of the Channel 2 to Channel 1 count rates will hereafter be defined as the "Soft" X-ray color, and the ratio of Channel 3 to Channel 2 count rates will be labeled as the "Hard" X-ray color.

3. RESULTS

The inclusion of a confirmed infrared bright state on 2010 May 24 rules out the 3.0125 day period of Paper I. Our reanalysis of all of the infrared bright times indicates that the true period of these events is 3.0367 ± 0.0006 days. This period is consistent with all detected outbursts back to the 1995 June 12 event discussed by Callanan et al. (2002), but not included in the period search analysis performed in Paper I. The new period, along with the observations of May 24, should be used to predict future brightening events for this object. Unfortunately, some ambiguity remains in the timing of these events as we have not yet determined the duration of these brightenings. The light curves presented in Paper I show that GX17+2 can stay bright for at least five hours. Until we can determine the mid-point of more than one of these events, the current ephemeris cannot be used to project the timing of events too far into the future. Thus, continued monitoring will be required to keep this ephemeris current.

3.1. Deriving the Spectral Energy Distribution of GX17+2

Due to the large pixel scale of the IRAC and MIPS imagers, it is impossible to deconvolve GX17+2 from the nearby field star NP Ser. Thus, to extract the true fluxes of GX17+2 from these observations, we needed to determine the nature of NP Ser. As has been reported elsewhere, NP Ser has a spectrum consistent with a G star, though there has been some difficulty in reconciling the colors and the values of the extinction for this spectral type. We plot the *UBVRIJHK* photometry of NP Ser in Figure 3, along with the first epoch (GX17+2 = off) IRAC 4.5 μm flux (the *U* through *J* photometry for NP Ser is from Naylor et al. 1991). The SED of NP Ser is completely consistent with being a G0V reddened by $A_V = 1.4$ mag. This puts NP Ser at a distance of 2 kpc, with a value for the extinction one might expect at this low galactic latitude ($b = +1.^\circ3$). Our infrared fluxes of NP Ser are listed in Table 2, where the *H*- and *K*-band data in this table are from the May 18 observations. The *H*- and *K*-band magnitudes we derive for NP Ser are consistent with those reported by Naylor et al. (1991).

The *Spitzer* fluxes of NP Ser have been subtracted from the IRAC fluxes for GX17+2 in the following discussion (as can be seen in Figure 3, the flux of NP Ser is irrelevant at 24 μm). The infrared fluxes of GX17+2 in outburst (for all epochs) are listed in Table 2. Note that none of these data are simultaneous, though the light curves from the two IRAC bandpasses (for both epochs) were contiguous. The data set presented in Paper I shows that the peak *K* magnitude of an outburst can vary by ±30% from event to event. We found a similar level of variability between the two epochs of IRAC observations. For example, the mean 3.6 μm flux for the first epoch was 1.68 mJy, while for the second epoch it was 1.04 mJy. Due to this variability, we have averaged the two epochs together to get mean fluxes in the two IRAC bands for producing its SED. The observed SED of GX17+2 during outburst is plotted in red in Figure 3.

It is well known that GX17+2 suffers from considerable extinction. For example, Naylor et al. (1991) argue that the observed X-ray halo implies an ("order of magnitude") extinction near $A_V \sim 14$ mag. We can also use the observed hydrogen column in the X-rays to estimate the extinction. The hydrogen column reported for GX17+2 varies with the spectral model fitted to the X-ray data, ranging from $\approx 1.7 \times 10^{22}$ up to $\approx 2.5 \times 10^{22}$ (see Di Salvo et al. 2000; Farinelli et al. 2005; Migliari et al. 2007). Using the calibration of the hydrogen column to visual extinction ($A_V = N_H/1.79 \times 10^{21}$) from Predehl & Schmitt (1995), we derive $9.7 \leqslant A_V \leqslant 14.0$ mag from the

[7] See http://heasarc.gsfc.nasa.gov/docs/xte/recipes/stdprod_guide.html.

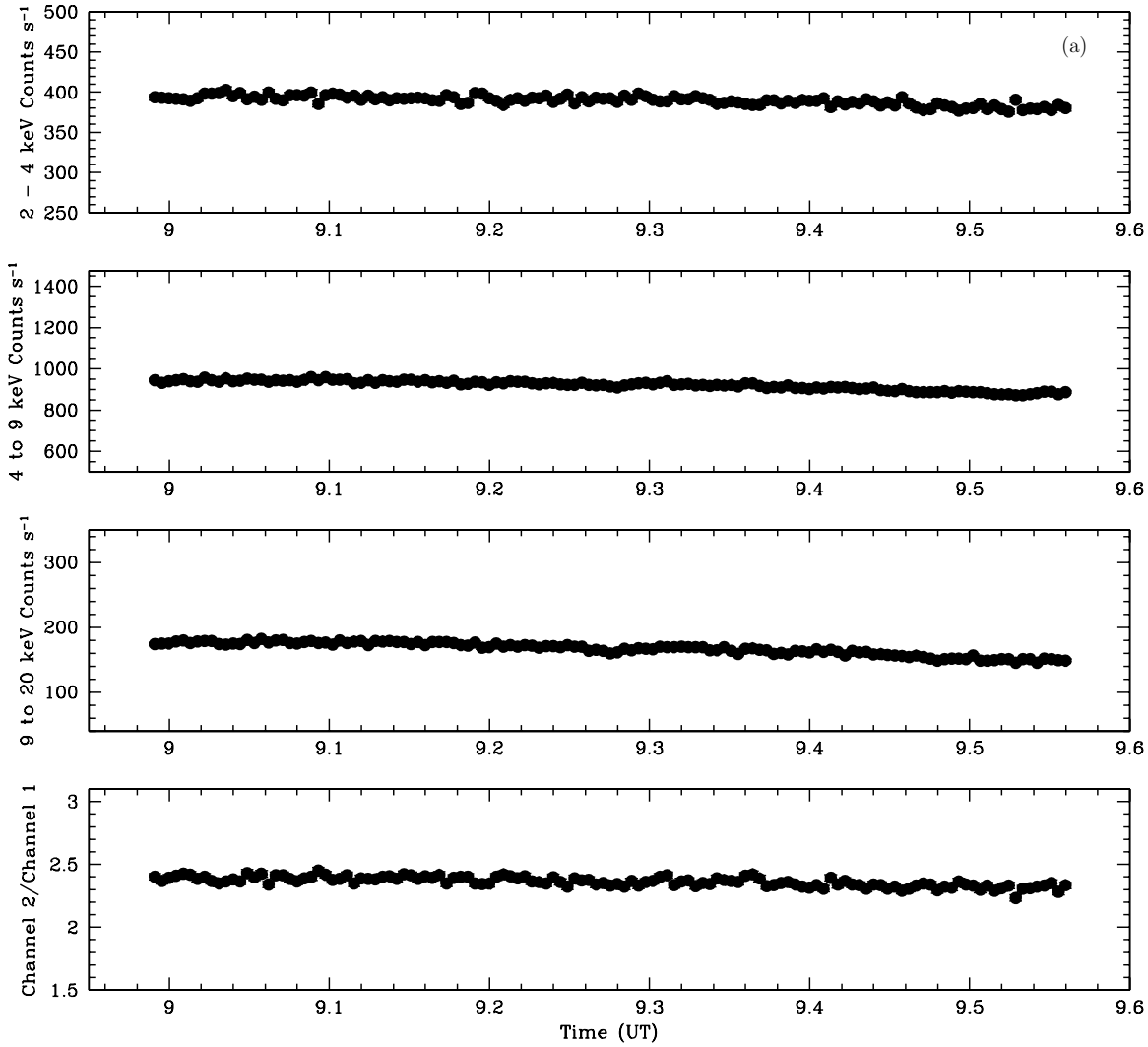

Figure 2. XTE light curves and hardness ratio for GX17+2 on (a) 2006 July 12, (b) 2010 May 18, and (c) 2010 May 21. *Y*-axes are the same in all three plots to highlight the fact that GX17+2 was on the flaring branch on May 18.

X-ray spectral fitting. We have dereddened the *H*- and *K*-band photometry using the standard relationships and corrected the *Spitzer* fluxes using the wavelength dependence of the extinction for the IRAC bandpasses as derived by Indebetouw et al. (2005), and for MIPS 24 μm from Flaherty et al. (2007). The results for the lower limit to the extinction, $A_V = 9.7$ mag, are the green circles plotted in Figure 3.

We can also examine the quiescent counterpart of GX17+2 to estimate its reddening by comparing it to the colors of the other Z-sources. As noted by Callanan et al. (2002), the object Deutsch et al. (1999) call star "A" is consistent with the position of the *K*-band counterpart for GX17+2. From these observations, GX17+2 in quiescence has $(J - H) = 1.7$ and $(H - K) = 1.5$. Using published photometry for GX13+1 (Charles & Naylor 1992), GX349+2 (Wachter & Margon 1996), and the 2MASS data for Sco X-1 and Cyg X-2, we plot the infrared color–color diagram for these four Z-sources in Figure 4. Using their observed hydrogen columns to estimate their extinctions, we find that the mean infrared colors of Z-sources are $\langle(J - H)\rangle = 0.17$ and $\langle(H - K)\rangle = 0.03$. To get the photometry of GX17+2 to approximate the mean Z-source color implies an extinction of $A_V = 17.5$. This value is much higher than inferred from the X-ray observations, and the resulting dereddened SED shown in Figure 3 (blue stars) has a peculiar shape requiring at least two components. It is not clear if this technique is a useful method for determining the extinction for GX17+2, especially given the non-simultaneous nature of the quiescent infrared photometry of GX17+2. It may indicate that the infrared colors of the quiescent GX17+2 are unlike the other Z-sources. Additional, near-simultaneous, deep, multi-band infrared observations are needed to resolve this issue.

Given the uncertain value for A_V, the uncertainties in the mid-IR reddening relationships, and the fact that the infrared brightenings vary by 30% from event to event, extracting the exact spectral form of a brightening event is not without its problems. But as shown in Figure 3, dereddened SEDs using $A_V \sim 10$ mag can be modeled with a single synchrotron spectrum. If the actual extinction is significantly larger than this, the spectrum begins to require a two-component model. Obviously, with only five data points, it would be meaningless to attempt to constrain two-component models. But even if such a model were in fact correct, the slope of a fit to the 4.5–24 μm fluxes ($f_\nu \propto \nu^{-0.7}$) would still suggest a synchrotron origin for much of the infrared luminosity. We examine the various scenarios for producing periodic synchrotron emission in Section 4.

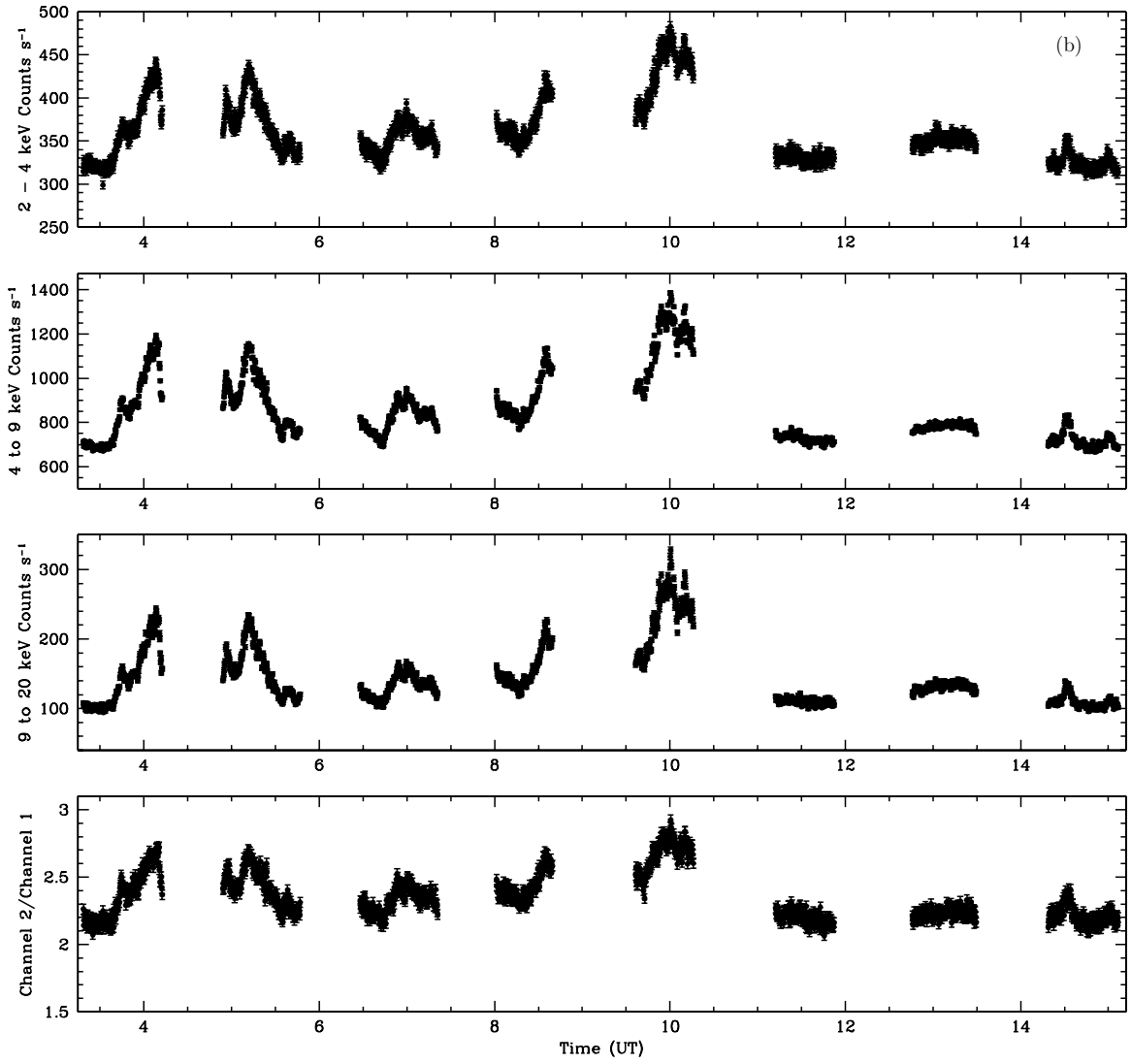

Figure 2. (Continued)

3.2. The Post-cryo IRAC Light Curves of GX17+2

To allow us to investigate the variability during the outbursts, we obtained two epochs of post-cryo IRAC observations, each spanning nearly 1.8 hr. These light curves, shown in Figure 5, demonstrate that there was considerable variability of the fluxes from GX17+2 during these observations, but there was no obvious rise or fall that would have indicated that we had caught the source near the beginning, or end, of a brightening event like those seen in three of the four *K*-band light curves presented in Paper I. It is clear, however, that GX17+2 is highly variable at the 40%–50% level in the mid-IR during these brightenings. During the first epoch of observation (October 20), the 4.5 μm light curve has three large flaring events, each lasting about 15 minutes. The 3.6 μm light curve, which was contiguous to the 4.5 μm data set, is more complex, with at least four large flares with durations of $\sim$10–15 minutes. There appear to be shorter-lived flares (e.g., at 18.3 UT), but the signal-to-noise ratio and temporal resolution are insufficient to quantify those events.

The light curves for the second epoch were slightly less variable. In the 4.5 μm light curve there were no well-defined flaring events, but several short-lived "dips" which appear to dominate the overall shape of the light curve. Four of these dips (between 18.25 and 18.75 UT) had nearly identical minima. The 3.6 μm light curve more closely resembled the first epoch data with three large flaring events. While the 4.5 μm light curve does appear to be slowly declining over the observed interval, the follow-on 3.6 μm light curve appears to be slowly rising. Thus, like the first epoch light curves, there is no evidence for an overall rising or falling to indicate we had caught GX17+2 near the start or end of a brightening event.

The *K*-band light curves presented in Paper I show similar amplitude flux variations as those in the mid-IR, but the time resolution of those light curves was insufficient to directly compare with the IRAC data set. The radio emission from GX17+2 is also highly variable, but none of the radio light curves presented for this source have sufficient temporal resolution to determine if similar scale features are observed. The *K*-band light curve of the black hole source GRS1915+105 shows events with similar amplitudes, though they are both slightly larger in size and longer in duration than the features we see in GX17+2. Fender et al. (1997) attribute the near-IR variations of that source to variations in the synchrotron emission from its jet. Fuchs et al. (2003) concluded that GRS1915+105 is highly variable at mid-IR wavelengths. The short-lived, large-scale mid-IR flares for GX17+2 can only reasonably be explained as due to synchrotron emission.

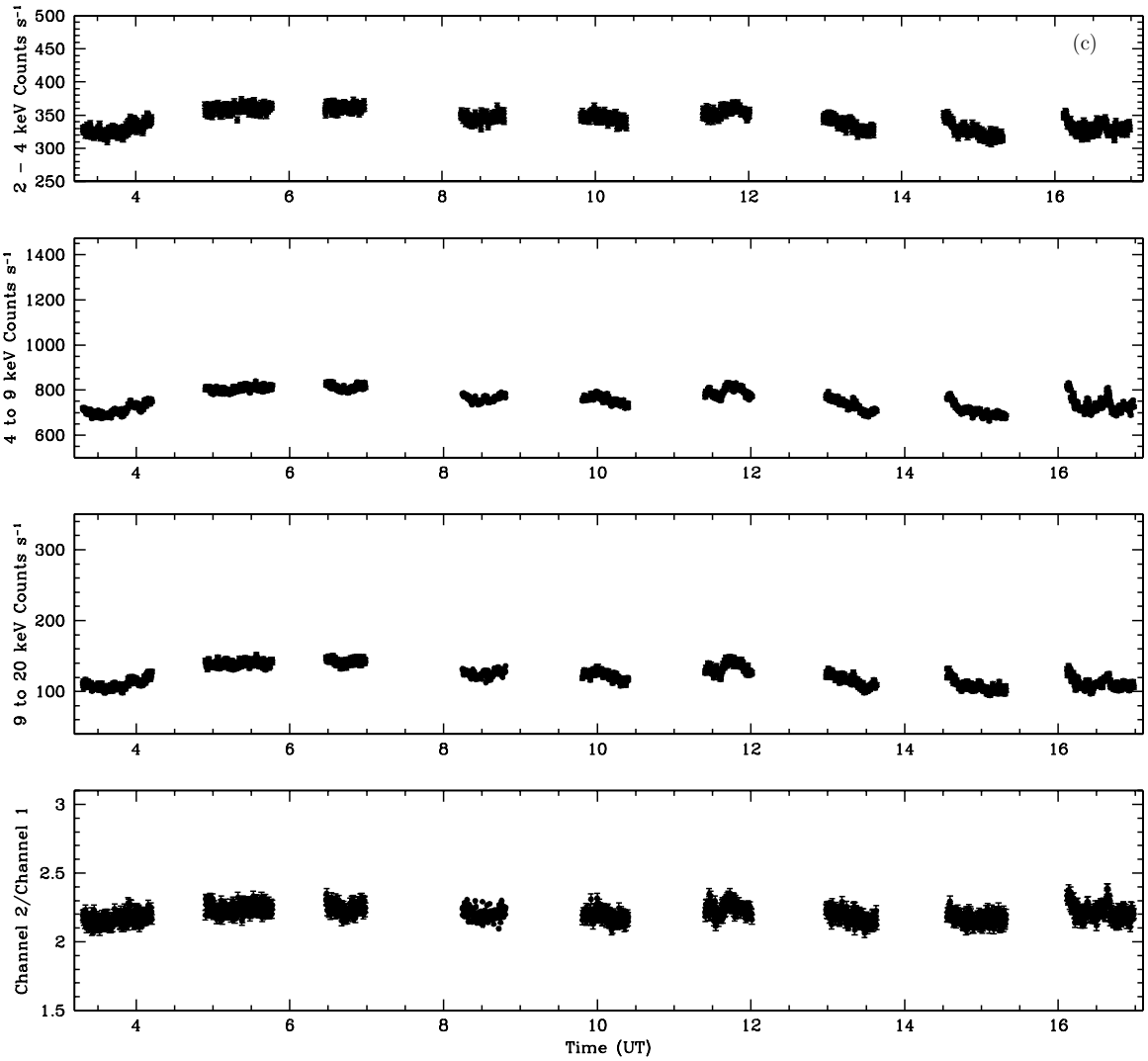

Figure 2. (Continued)

Table 2
Fluxes for NP Ser and GX 17+2

Object	H_{2MASS} (mag)	K_{2MASS} (mag)	3.6 μm (mJy)	4.5 μm (mJy)	24 μm (mJy)
NP Ser	14.56 ± 0.02	14.43 ± 0.02	0.52[a]	0.332 ± 0.005	0.01[a]
GX17+2	17.09 ± 0.04[b]	15.35 ± 0.02[b]	1.676 ± 0.004	2.068 ± 0.004	5.61 ± 0.01[c]
GX17+2	...	...	1.046 ± 0.003	1.842 ± 0.004	...

Notes.
[a] These flux densities were estimated using the Star-PET tool located at http://ssc.spitzer.caltech.edu/warmmission/propkit/pet/starpet/index.html, using the *K*-band magnitude of NP Ser.
[b] These data are for 2010 May 24.
[c] The MIPS observation occurred on 2008 October 10.

4. DISCUSSION

It has become abundantly clear that the accretion disks surrounding compact objects are capable of spawning relativistic jets. X-ray binaries with black hole primaries have long been known to harbor such jets. There is now considerable evidence that X-ray binaries with neutron star primaries are also capable of launching jets. Only recently, with the launch of *Spitzer*, has it been possible to confirm that emission from the jets of X-ray binaries extends into the near-IR portion of the spectrum. For example, Gallo et al. (2007) and Gelino et al. (2010) present mid-IR photometry of quiescent X-ray binaries with black hole primaries showing that they have strong jet emission, even at very low accretion rates. Fits to the IRAC/MIPS fluxes indicate optically thin synchrotron spectra for those objects. In the black hole system GRS1915+105, the synchrotron jets have been imaged in the near-IR (Eikenberry & Fazio 1997). This object has highly variable near- and mid-IR emission that is correlated with its X-ray and/or radio emission (see Fuchs et al. 2003, and references therein). Migliari et al. (2006) show that the

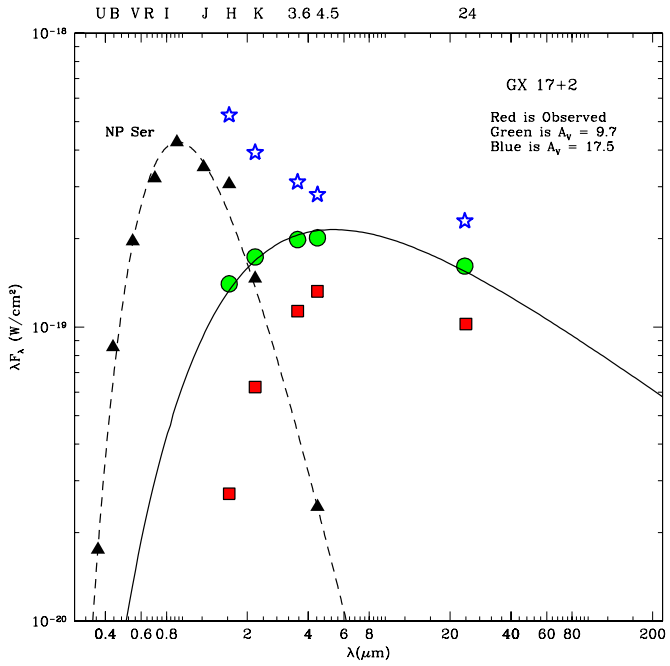

Figure 3. Observed optical and infrared photometry of NP Ser (black triangles) and the observed infrared photometry of GX17+2 during a brightening (red squares). The SED of NP Ser has been fitted with a 6000 K blackbody reddened by 1.4 mag (dashed line). The data for GX17+2 dereddened by $A_V = 9.7$ mag are shown as green circles and by $A_V = 17.5$ mag as blue stars. One possible synchrotron model (see http://www.jca.umbc.edu/~markos/cs/comptontoys/comptontoys.html) has been plotted as a solid line, suggesting that the source luminosity peaks in the mid-IR.

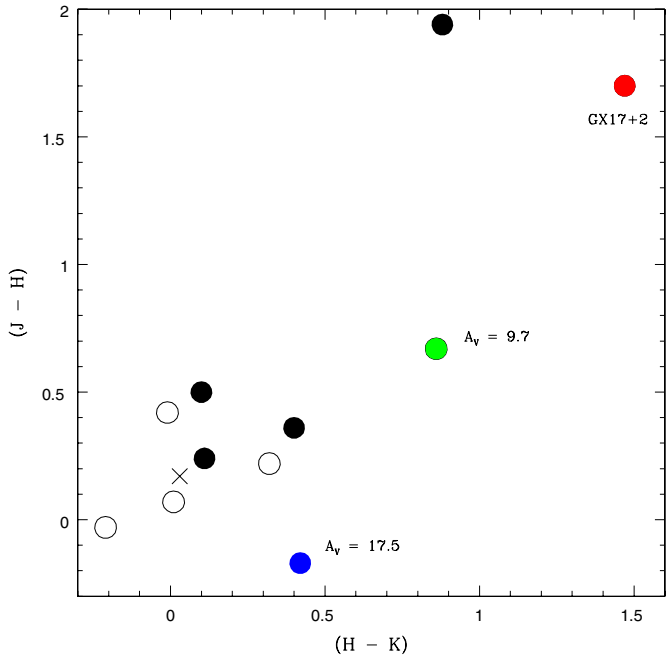

Figure 4. Infrared color–color plot for Z-sources. The observed colors are shown as filled black circles and the dereddened colors are open circles. The mean color for Z-sources is indicated by the cross. The observed quiescent color of GX17+2 is indicated in red and the dereddened colors (as labeled) are in green and blue.

X-ray binary 4U 0614+091, an "Atoll" source with a neutron star primary, also has an optically thin synchrotron spectrum in the mid-IR. Even cataclysmic variables with white dwarf primaries have transient synchrotron jet emission (Körding et al. 2008; Harrison et al. 2010). Thus, it is not a surprise that GX17+2 also exhibits an infrared SED that is consistent with synchrotron emission. Given the strong evidence for a relativistic radio jet in this system, we conclude that the IR brightenings are associated with this jet. The curious aspect is how this emission can be precisely periodic.

One important aspect for understanding the behavior of this source is to establish whether there is any correlation between its X-ray emission, and the occurrence of an IR brightening. As discussed in Bailyn & Grindlay (1987), analysis of X-ray data has resulted in a number of possible periodicities for GX17+2 ranging from 1.4 hr up to 6.5 days. Bandyopadhyay et al. (2002) searched for periodic X-ray emission in an *RXTE* All-Sky Monitor light curve of GX17+2 spanning 200 days, but were unable to find any significant periodicities.

We have been able to obtain two epochs of simultaneous X-ray/IR observations of GX17+2 when it was predicted to be bright. Of these two data sets, the one for 2006 July 12 has GX17+2 as IR bright, but for the other, 2010 May 18, GX17+2 was undetected. We have produced an X-ray color–color plot for the simultaneous near-IR/*RXTE* observations in Figure 6. For the 2006 epoch (blue), GX17+2 was clearly well down the NB of the Z. The *RXTE* data for the 2010 observation (green) found GX17+2 to be on the FB. Unfortunately, we have not sampled very much of the X-ray behavior of GX17+2 with just two epochs of data. Because of our improved confidence in the ephemeris, however, we can go back and investigate whether the X-ray behavior of GX17+2 during predicted IR brightening events was at all unusual. We have run the ephemeris back 11 years to identify other *RXTE* observations of GX17+2 that occurred near predicted bright times, and extracted and reduced those data to investigate the X-ray state of GX17+2. As shown in Paper I, GX17+2 can stay bright for at least five hours in the near-IR. Thus, in the following, we will consider all X-ray data within ±2.5 hr of the predicted outburst time as being simultaneous to the IR bright phase. We plot the *RXTE* data that were obtained within ±2.5 hr of a predicted IR brightening in red in Figure 6. Data obtained on the same days, but outside the bright time window (sometimes as much as 10 hr later), are plotted with black crosses. We conclude that there is no obvious correlation between a predicted IR bright phase and the position of GX17+2 in its Z-diagram.

If the IR brightenings are to be attributed to the detection of the synchrotron jet in GX17+2, this requires the jet to be active most of the time. The only time a predicted IR brightening was not detected occurred when GX17+2 was on the FB. If this is universally true, then the analysis of the data plotted in the Z-diagram of Figure 6 shows that GX17+2 will be on the FB 30% of the time, and thus we would expect that IR brightenings would not be observed for this fraction of events. Given that only 15 IR brightenings have been observed in total, and only 5 predicted events were observed after the development of an accurate ephemeris, it is not too surprising that there was only 1 occurrence when GX17+2 was not observed to be IR bright.

Migliari et al. (2007) showed that a hard X-ray tail is clearly present when GX17+2 is on, or near, the HB. During this time, the radio emission from GX17+2 is the strongest, indicating the presence of a synchrotron jet. They found that both the radio emission and the hard X-ray tail became less prominent as the source evolved down the NB toward the FB. In our analysis of the Z-diagram for GX17+2, we find that this object only spends 20% of its time on the HB. If being on the HB was the only condition for the presence of mid-IR synchrotron source, then

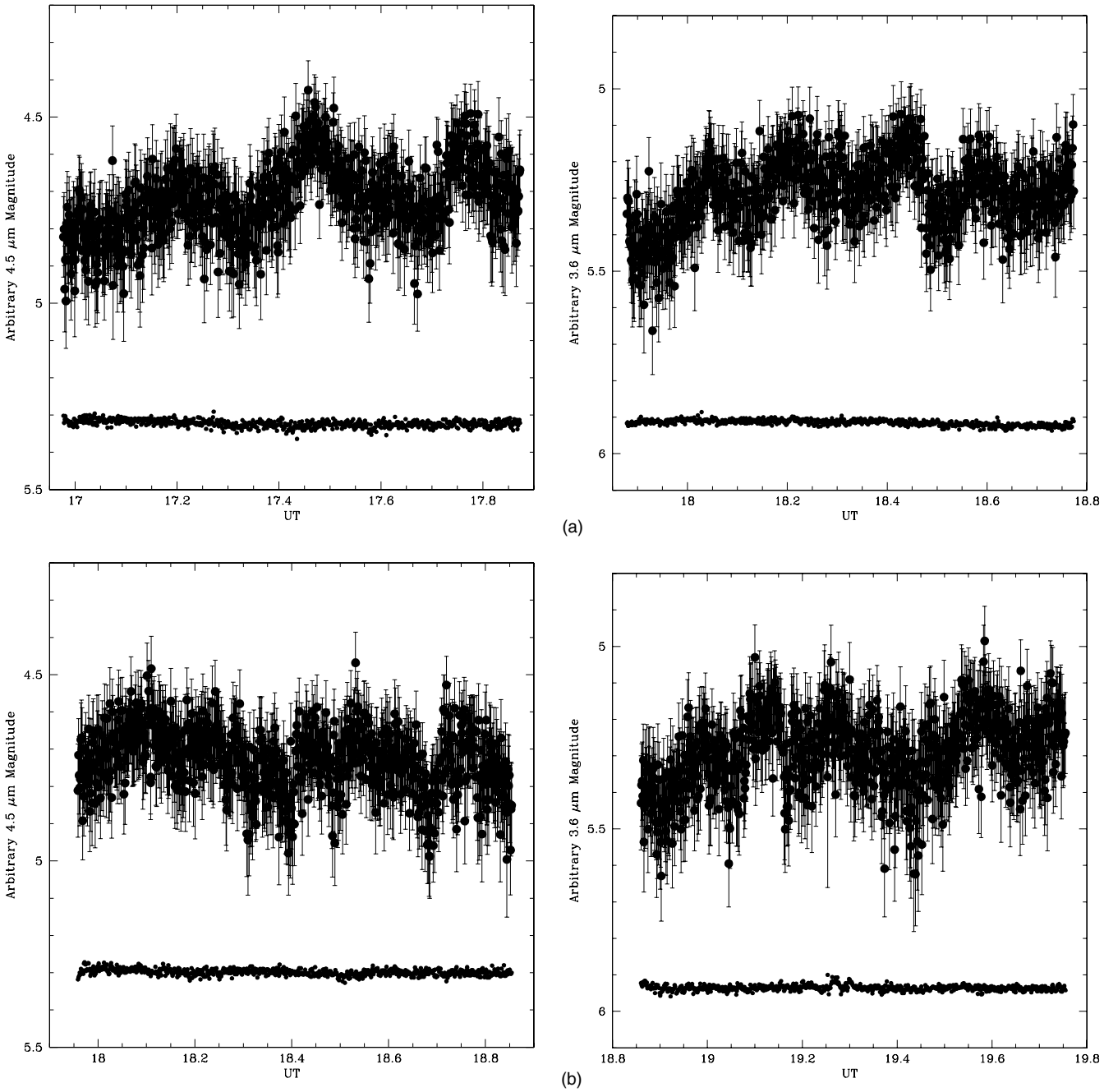

Figure 5. IRAC 4.5 μm (left) and 3.6 μm (right) light curves for (a) 2009 October 20 and (b) 2009 November 1. The light curve of one of the bright reference stars used for the differential photometry is plotted at the bottom in all figures.

we should not have successfully observed as many predicted brightening events as we have. This indicates to us that both the mid-IR and radio emission are from the same source, and that both are present well down the NB.

4.1. Comparing GX17+2 to Cir X-1

Cir X-1 is an enigmatic X-ray binary that for decades has eluded precise classification. Recently, however, the resumption of typical Type I X-ray bursts after a 25 yr hiatus (Linares et al. 2010), along with the identification of evolution in the X-ray color–color diagram indicating typical Z-source behavior (Shirey et al. 1999), has lead to the firm conclusion that the compact object in Cir X-1 is a neutron star. One of the properties that makes Cir X-1 unique is the large-scale infrared outbursts that occur every 16.58 days. As shown by Glass (1994), Cir X-1 brightens by about two magnitudes in the *K* band, taking 1.5 days to rise to maximum light, and then declining back to quiescence in ∼3 days. The infrared events are exactly correlated with radio flares that occur at the same phase ("phase 0") of the 16.58 days ephemeris (Stewart et al. 1991). In addition to these properties, Cir X-1 clearly has a relativistic jet that has been detected in both the X-ray (Sell et al. 2010) and radio (Fender et al. 2004). A hard X-ray tail also appears to be present when Cir X-1 is near phase 0 (Iaria et al. 2001).

The model evolved for Cir X-1 is that it is an eccentric binary ($e \geqslant 0.4$) consisting of a main-sequence/subgiant star and a weakly magnetized neutron star (Johnston et al. 1999, and references therein). At the periastron passage, identified with

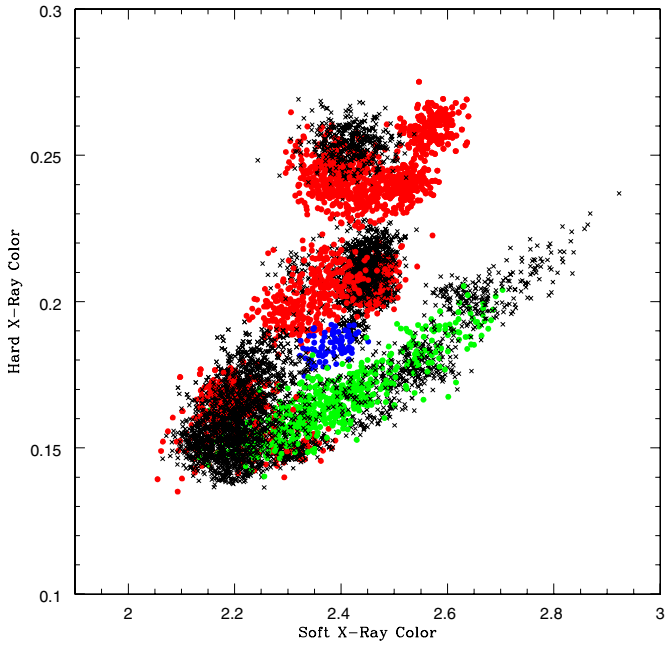

Figure 6. X-ray color–color plot for GX17+2 for times when GX17+2 was predicted to be IR-bright. The "Z" for GX17+2 can be clearly seen, with the HB defined as the region of the diagram centered at a value for the soft color of ∼2.5, but with hard color ⩾0.22. The FB is the diagonal region delineated by the data in the lower right-hand part of the plot. The NB connects the HB to the FB. The green (2010 May 18) and blue (2006 July 12) circles indicate the results for when strictly simultaneous data were obtained which confirmed the IR state of GX17+2. The red points detail previous X-ray observations that occurred during predicted IR-bright times. All X-ray data obtained within ±2.5 hr of a predicted IR-bright time are considered to have occurred during a brightening. The data plotted with black crosses were obtained on the same day as a predicted event, but were obtained outside the 2.5 hr bright time window.

the phase 0 defined by the radio ephemeris, there is increased mass transfer to the neutron star. Presumably, the dumping of this mass into an accretion disk around the neutron star generates the X-ray, infrared, and radio outbursts. The difficulty with associating Cir X-1 with GX17+2 is that the latter always looks like a Z-source, while Cir X-1 only looks like a Z-source some of the time. In addition, there is no evidence for changes in the X-ray properties of GX17+2 during its infrared maxima. Thus, while the two objects exhibit similar low energy behavior, the differences at high energy appear to rule out episodic mass transfer events from a highly eccentric binary as the cause for the brightenings of GX17+2.

4.2. Are the Infrared Brightenings of GX17+2 due to a Precessing or a Nutating Jet?

The perfectly periodic behavior of the IR brightenings suggests the possibility of either the precession or the nutation of a jet across our line of sight as the source for these events. The orbital period of GX17+2 is unknown. However, orbital periods have been established for two Z-sources: Sco X-1 (18.9 hr; Gottlieb et al. 1975; Vanderlinde et al. 2003) and Cyg X-2 (9.8 days; Casares et al. 1998). In addition, a 21.85 hr period has been reported for GX349+2 (Wachter & Margon 1996). It is reasonable to assume that the orbital period of GX17+2 is on the order of days. The standard model for the accretion process in Z-sources assumes that the secondary star fills its Roche lobe, and thus the eccentricity of the binary system must be near zero. Even if this were not the case, the apsidal motions of an eccentric binary with an orbital period near a day would be very slow. In the eclipsing B-star binary DI Her, where $e = 0.489$ and $P_{\rm orb} = 10.55$ days, the classical apsidal motion is on order of 10^4 yr (Company et al. 1988). If the rotational spin axes of the two stellar objects in the binary are not aligned, the classical apsidal motion is modified. In the case of DI Her, the misaligned spins result in a slower precession than in the pure apsidal case (Company et al. 1988). In DI Her, there is an additional component of precession due to relativistic effects, but this relativistic precession is approximately the same size as the classical effect (though there are binaries where the relativistic term dominates; see Wolf et al. 2010). Lai et al. (1995) have examined the spin–orbit interaction for neutron star/main-sequence binaries and find similar, very slow precession rates for these types of systems. It is obvious that precession of an isolated Z-source binary is always going to be much, much longer than the orbital period.

The presence of a third body in the system can lead to much more rapid precession. For example, in the high-mass eclipsing binary system IU Aur ($P_{\rm orb} = 1.8$ days), a third body orbits with a period of 293 days. This induces a precession period of 335 yr for the orbit of the eclipsing stars (Drechsel et al. 1994). This is an order of magnitude more rapid precession than seen in isolated, eccentric binaries. Mazeh & Shaham (1976) show that to first order, the angular frequency of the induced precession on the tighter binary in a triple star system is $\omega = \frac{m_3}{m_1+m_2}(\frac{a_1}{a_2})^3\Omega\eta$, where m_1, m_2, and m_3 are the masses of the three stars, a_1 is the semimajor axis of the inner binary, a_2 is the semimajor axis of the orbit of the distant third star, and Ω is the angular frequency of the tight binary. η is a geometrical factor that is close to one, unless the third star has a large eccentricity (large η), or the orbit of the third body is highly non-coplanar (small η). Mazeh & Shaham (1976) use λ Tau as an example, where the inner binary has a period of 4 days, and a total mass of 10 $M_\odot$, orbited by a solar mass object with $P_{\rm orb} = 33$ days. The precession period in this case is 10 yr. It is clear that if the third component were to have a significant mass, the induced precession could be on order of the inner binary star period.

Using the equations in Mazeh & Shaham (1976) we can roughly estimate the nature of a possible third body in GX17+2. Using the parameters for the Cyg X-2 system, $P_{\rm orb} = 9.8$ days and $m_1 + m_2 = 2.291\ M_\odot$ (Casares et al. 2010), and using a value of $a_1/a_2 \geqslant 3$ (Donnison & Mikulskis 1995) required to have a stable triple star system, we find that $m_3 = 6.4/\eta\ M_\odot$. For a coplanar orbit with an eccentricity of $e = 0.5$, $\eta \sim 1.5$. Given that the orbital period of GX17+2 is unknown, we cannot rule out that a third body is causing the precession which results in the periodic transiting of a jet across our line of sight. Such an object might also explain why the quiescent colors of GX17+2 are unlike the other Z-sources.

The case for the precession of a warped/misaligned accretion disk in GX17+2 system as the driver for jet motion is much more relevant. In pre-main-sequence star binaries, it is frequently observed that the jets appear to be precessing (cf. Eisloffel et al. 1996). Bate et al. (2000) describe how an accretion disk that is misaligned with the plane of the binary can precess with a period that is exactly one-half of the orbital period (the "$m = 2$ tidal component"). This type of motion has been used to explain the 6.28 days nutational oscillations in SS433, a high-mass X-ray binary that has an orbital period of 13.1 days (Fabrika 2004). In SS433, however, the wobble angle of the nutation is only 2.°8, with a jet that has an opening angle of ⩽1.°4 (Fabrika 2004). This type of nutational movement would require the orbital inclination of GX17+2 to be very close to 90°. It is interesting

to note that Ponman (1982) did report an X-ray periodicity for GX17+2 with a period of 6.437 ± 0.02 days, not too different from twice the IR periodicity.

It is the longer period precession of the jet in SS433 that may be more applicable to GX17+2. In SS433, the accretion disk around the compact object is strongly self-irradiated. This irradiation causes the outer edges of the disk to warp out of the orbital plane and to precess with a period of 162 days. As discussed in Begelman et al. (2006), this precession must be communicated to the inner parts of the disk to be imparted on the regions where the jet is launched. Begelman et al. (2006) propose that the mass-transfer rate in SS433 is "hyper-Eddington," leading to a strong disk wind that helps collimate the jets. The precession of the warped disk is then communicated directly to the jets by this wind. The half-angle of the cone on which the jets move due to this precession is 20°, removing the requirement of a special alignment of our line of sight with the binary orbital plane. A rate of precession some 10 times the orbital period would mean an orbital period for GX17+2 of 7 hr, but this is completely consistent with the orbital periods of numerous LMXBs (see Ritter & Kolb 2003).

Since SS433 remains unique, it is dangerous to use it as an analog to GX17+2. Ogilvie & Dubus (2001) investigated the warping and precession of accretion disks in a wide range of X-ray binaries. To get significant warping in systems like GX17+2 requires a higher disk viscosity ("α"), or a higher accretion efficiency ($L_*/\dot{m}c^2$), than expected. The fact that disk precession has been invoked to explain the 78 days superorbital period for Cyg X-2 (Wijnands et al. 1996, though see Larwood 1998) suggests that some Z-sources may have warped disks. In Cyg X-2 the ratio of the superorbital period to the orbital period is eight, which would require GX17+2 to have an orbital period of 9.6 hr if their binary mass ratios were similar.

5. CONCLUSIONS

GX17+2 is unique among the Z-sources in that it exhibits ∼3 mag brightening events in the *K* band. Bornak et al. (2009) found that these events were periodic. Using that ephemeris, we have obtained additional near- and mid-IR observations that confirm the periodicity of these events, though we have revised the period of these events to 3.0367 days. This new period allows us to explain all of the reported brightenings of this object. This ephemeris was used to obtain *Spitzer* observations of this source which showed that the SEDs of these events have a synchrotron spectrum. It is now clear that nearly all of the Z-sources, including GX17+2, have relativistic synchrotron jets. None of them, however, exhibit perfectly periodic jet emission. There seem to be two viable explanations for these events: induced precession due to a third body in the system, or perhaps the accretion disk is warped, and its precession is communicated to the inner regions where the jet is actually launched through a strong disk wind.

It is clear that GX17+2 warrants additional multi-wavelength campaigns to fully understand its behavior. Given the long period between these events, ground-based campaigns from a single location have only a few days each year where the source allows for significant coverage of a brightening event. From northern latitudes, it is extremely difficult to obtain a light curve that would allow one to determine the full duration of these events. This uncertainty makes continued monitoring essential to keep the ephemeris current. Simultaneous radio, infrared, and X-ray observations of several of these brightening events are essential for conclusive determination of their nature.

REFERENCES

Bailyn, C. D., & Grindlay, J. E. 1987, ApJ, 312, 748
Bandyopadhyay, R. M., Charles, P. A., Shahbaz, T., & Wagner, R. M. 2002, ApJ, 570, 793
Bate, M. R., Bonnell, I. A., Clarke, C. J., Lubow, S. H., Ogilvie, G. I., Pringle, J. E., & Tout, C. A. 2000, MNRAS, 317, 773
Begelman, M. C., King, A. R., & Pringle, J. E. 2006, MNRAS, 370, 399
Bornak, J., McNamara, B. J., Harrison, T. E., Rupen, M. P., Bandyopadhyay, R. M., & Wachter, S. 2009, ApJ, 701, L110 (Paper I)
Callanan, P. J., et al. 2002, ApJ, 574, L143
Casares, J., Charles, P., & Kuulkers, E. 1998, ApJ, 493, L39
Casares, J., Gonzalez Hernandez, J. I., Israelian, G., & Rebolo, R. 2010, MNRAS, 401, 2517
Charles, P. A., & Naylor, T. 1992, MNRAS, 255, 6
Company, R., Portilla, M., & Gimenez, A. 1988, ApJ, 335, 962
Deutsch, E. W., Margon, B., Anderson, S. F., Wachter, S., & Goss, W. M. 1999, ApJ, 524, 406
Di Salvo, T., et al. 2000, ApJ, 554, L119
Donnison, J. R., & Mikulskis, D. F. 1995, MNRAS, 272, 1
Drechsel, H., Haas, S., Lorenz, R., & Mayer, P. 1994, A&A, 284, 853
Eikenberry, S. S., & Fazio, G. G. 1997, ApJ, 475, L53
Eisloffel, J., Smith, M. D., Davis, C. J., & Ray, T. P. 1996, AJ, 112, 2086
Fabrika, S. 2004, Astrophys. Space Phys. Rev., 12, 1
Farinelli, R., Frontera, F., Zdziarski, A. A., Stella, L., Zhang, S. N., van der Klis, M., Masetti, N., & Amati, L. 2005, A&A, 434, 25
Fazio, G. G., et al. 2004, ApJS, 154, 39
Fender, R., Wu, K., Johnston, H., Tzioumis, T., Jonker, P., Spencer, R., & van der Klis, M. 2004, Nature, 427, 222
Fender, R. P., Pooley, G. G., Brocksopp, C., & Newell, S. J. 1997, MNRAS, 290, 65
Flaherty, K. M., Pipher, J. L., Megeath, S. T., Winston, E. M., Gutermuth, R. A., Muzerolle, J., Allen, L. E., & Fazio, G. G. 2007, ApJ, 663, 1069
Fuchs, Y., Mirabel, I. F., & Claret, A. 2003, A&A, 404, 1011
Gallo, E., Migliari, S., Markoff, S., Tomsick, J. A., Bailyn, C. D., Berta, S., Fender, R., & Miller-Jones, J. C. A. 2007, ApJ, 670, 600
Gelino, D. M., Gelino, C. R., & Harrison, T. E. 2010, ApJ, 718, 1
Glass, I. 1994, MNRAS, 268, 742
Gottlieb, E. W., Wright, E. L., & Liller, W. 1975, ApJ, 195, L33
Harrison, T. E., Bornak, J., Rupen, M. P., & Howell, S. B. 2010, ApJ, 710, 325
Hasinger, G., van der Klis, M., Ebisawa, K., Dotani, T., & Mitsuda, K. 1990, A&A, 235, 131
Iaria, R., Burderi, L., Di Salvo, T., La Barbera, A., & Robba, N. R. 2001, ApJ, 547, 412
Indebetouw, R., et al. 2005, ApJ, 619, 931
Jackson, N. K., Church, M. J., & Balucinska-Church, M. 2009, A&A, 494, 1059
Johnston, H. M., Fender, R., & Wu, K. 1999, MNRAS, 308, 415
Körding, E., Rupen, M., Knigge, C., Fender, R., Dhawan, V., Templeton, M., & Muxlow, T. 2008, Science, 320, 1318
Lai, D., Bildsten, L., & Kaspi, V. M. 1995, ApJ, 452, 819
Larwood, J. 1998, MNRAS, 299, L32
Lin, D., Remillard, R. A., & Homan, J. 2009, ApJ, 696, 1257
Linares, M., et al. 2010, ApJ, 719, L84
Mazeh, T., & Shaham, J. 1976, ApJ, 205, L147
Migliari, S., & Fender, R. P. 2006, MNRAS, 366, 79
Migliari, S., Tomsick, J. A., Maccarone, T. J., Gallo, E., Fender, R. P., Nelemans, G., & Russell, F. M. 2006, ApJ, 643, L41
Migliari, S., et al. 2007, ApJ, 671, 706
Naylor, T., Charles, P. A., & Longmore, A. J. 1991, MNRAS, 252, 203
Ogilvie, G. I., & Dubus, G. 2001, MNRAS, 320, 485
Penninx, W., Lewin, W. H. G., Zijlstra, A. A., Mitsuda, K., van Paradijs, J., & van der Klis, M. 1988, Nature, 336, 146
Ponman, T. 1982, MNRAS, 200, 351
Predehl, P., & Schmitt, J. H. M. M. 1995, A&A, 293, 889
Rieke, G. H., et al. 2004, ApJS, 154, 25
Ritter, H., & Kolb, U. 2003, A&A, 404, 301
Sell, P. H., et al. 2010, ApJ, 719, L194
Shirey, R. E., Bradt, H. V., & Levine, A. M. 1999, AJ, 517, 472
Stewart, R. T., Nelson, G. J., Penninx, W., Kitamoto, S., Miyamoto, S., & Nicholson, G. D. 1991, MNRAS, 253, 212
Vanderlinde, K. W., Levine, A. M., & Rappaport, S. A. 2003, PASP, 115, 739
Vrtilek, S. D., Raymond, J. C., Garcia, M. R., Verbunt, F., Hasinger, G., & Kurster, M. 1990, A&A, 235, 162
Wachter, S., & Margon, B. 1996, AJ, 112, 2684
Wijnands, R. A. D., Kuulkers, E., & Smale, A. P. 1996, ApJ, 473, 45
Wolf, M., Claret, A., Kotkova, L., Kuakova, H., Kocian, R., Brat, L., Svoboda, P., & Smelcer, L. 2010, A&A, 509, 18